An Integrated SWIPT Receiver using Non-Coherent Detection Schemes

Eleni Goudeli, Constantinos Psomas, and Ioannis Krikidis
KIOS Research and Innovation Center of Excellence,
Department of Electrical and Computer Engineering, University of Cyprus, Cyprus
Email: {egoude01, psomas, krikidis}@ucy.ac.cy

***Abstract*—In this paper, we investigate non-coherent detection schemes, for the integrated simultaneous wireless information and power tranfer (SWIPT) receiver. Firstly, we study a symbol by symbol (SBS) detection, while optimization of the transmitted energy pulses, enhances the performance of the receiver, in terms of symbol error rate (SER). In addition, by exploiting the channel coherence time, over N transmitted energy pulses, we study sequential detection and introduce an integrated SEQ-MLSD decoder. With the use of sophisticated techniques such as Viterbi-type trellis-search algorithm and strategic-store strategy, we simplify the complexity of the sequential detection and overcome the error floor problem. Simulation results along with theoretical bounds are provided, validating the enhanced performance of our solution. The proposed sequential decoding scheme outperforms in terms of SER, the integrated SBS decoder and the conventional power-splitting SWIPT receiver, without degrading the energy harvested.**

***Keywords*—SWIPT, integrated receiver, sequential decoding, non-coherent detection.**

I. Introduction

Simultaneous wireless information and power transfer (SWIPT) is a fundamental architecture in wireless powered communications, where radio-frequency (RF) signals simultaneously convey data and energy to devices. Due to practical constraints, SWIPT cannot be performed from the same received signal without losses, so practical implementations split the received signal in two parts, where one part is used for information transfer and another part is used for power transfer [1]. In the new era of internet of things and machine type communications, there will be a need for massive deployment of smart devices and vast amount of information exchange, making it impractical, even impossible, to individually recharge/control all these devices on a regular basis [2]. Towards this technological evolution, SWIPT technology is of significant importance for energy supply and information exchange.

Regarding the SWIPT concept, Varshney first proposed the idea of transmitting information and energy simultaneously in [3]. In [4], Grover and Sahai extended the work to frequency-selective channels with additive white Gaussian noise (AWGN). In [5], a novel design of a SWIPT receiver was proposed, in which the information decoding and the energy harvesting circuits are integrated. The replacement of the active RF to baseband conversion with a passive rectifier operation, has as a direct result the reduction of the energy cost for information decoding. Given the nature of the integrated architecture, decoding of the transmitted information is succeeded, by detecting the power variation in the received signal.

In [6], a SWIPT solution with the use of integrated receiver and precoding on the energy patterns is presented. However, such a solution relies on the availability of channel state information (CSI) at the receiver, resulting to a coherent decoding scheme. Coherent techniques are a challenging task, since the source needs to periodically send training symbols, which incurs an increased signaling overhead and processing burden [7]. On the other hand, with the use of non-coherent techniques, the receiver's complexity is reduced at the expense of a decreased spectral efficiency. In the literature, but in different contexts, there are studies for non-coherent detection techniques, which can result in an enhanced symbol error rate (SER) [8], [9], without profoundly increasing the complexity at the receiver side. Such techniques are generalized likelihood ratio test-maximum likelihood sequence detection (GLRT-MLSD), Viterbi-type trellis-search algorithm and selective store strategy (SS-ST).

We herein achieve SWIPT using an integrated receiver with non-coherent information decoding, succeeding an enhanced performance in terms of SER and energy harvested. To the best of our knowledge, there has not been a similar study in SWIPT literature. First, we analyze the symbol by symbol (SBS) detection, based on an equi-spaced pulse energy modulation (PEM) scheme. In addition, we optimize the pattern of the transmitted energy pulses with and without a level of power sensitivity at the side of the receiver [10]. Following this, we enhance the SER performance, by proposing a sophisticated sequential decoding scheme. More specifically, with the use of GLRT-MLSD and Viterbi-type trellis-search algorithm, we manage to diminish the computational complexity originated from the sequential detection and finally propose a simplified decision rule. Furthermore, we show that with the use of SS-ST, our proposed integrated decoder, denoted as integrated SEQ-MLSD, can overcome the error floor problem. Simulation

This work was supported by the European Union's Horizon 2020 research and innovation programme under grant agreement No 739551 (KIOS CoE), by the Government of the Republic of Cyprus through the Directorate General for European Programmes, Coordination and Development, and by the Research Promotion Foundation, Cyprus under the project COM-MED with pr. no. KOINA/ERANETMED/1114/03.

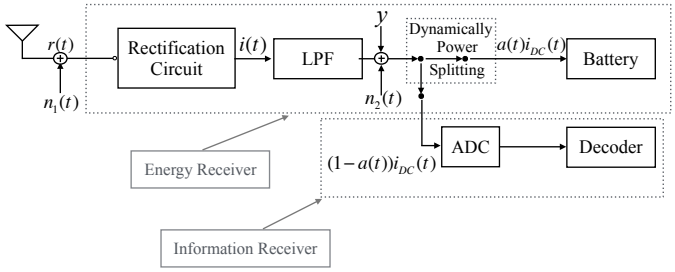

Fig. 1. Architecture of the integrated receiver.

results match the theoretical ones, thus validating our study on an innovative sequential and non-coherent decoder, which enables low values of SER and high energy harvested.

The rest of this paper is organized as follows: Section II presents the system model. In Section III, we present the SBS decoding, while in Section IV, the sequential decoding is described. Finally, the numerical results are presented in Section V, and the paper is concluded in Section VI.

Notation: Lowercase boldface letters denote vectors; $P(X)$ denotes the probability of the event X and $\mathbb{E}[X]$ represents the expected value of X; $\mathrm{erfc}\,(x) = \frac{2}{\sqrt{\pi}} \int_x^\infty e^{-t^2} dt$, $\mathrm{erf}\,(x) = 1 - \mathrm{erfc}\,(x)$ denote the complementary error function and the error function, respectively.

II. System Model

We consider an integrated information and energy receiver, as shown in Fig. 1, for a single input single output wireless link. At the transmitter side a baseband signal $x(t)$ is transmitted, with $\mathbb{E}[x^2(t)] = 1$. The modulation scheme used by the transmitter is PEM, with M energy levels. We design our energy pulse based symbol alphabet, based on equi-spaced amplitudes as in [6]. Specifically, we assume that a set of M symbols $x_i \in \{1d, 2d, \ldots, Md\}$, are mapped to each energy level, where d is the distance between the energy pulse based symbols. Therefore, we have

$$\mathbb{E}[x^2(t)] = \frac{1}{M} \sum_{i=1}^{M} x_i^2 = \frac{d^2}{6}(M+1)(2M+1) = 1, \quad (1)$$

which results in

$$d = \sqrt{\frac{6}{(M+1)(2M+1)}}. \quad (2)$$

The baseband signal is then up-converted to generate an RF signal, which is transmitted over a Rayleigh fading channel. The received complex signal $r(t)$ is given by [5]

$$r(t) = \sqrt{E_{\mathrm{ave}} h} x(t) + n_1(t), \quad (3)$$

where E_{ave} is the average transmitted power, $\sqrt{h}$ is the channel coefficient, modeled as complex Gaussian random variable with zero mean and unit variance. We assume that CSI is not available at the receiver and non-coherent detection is applied. Finally, $n_1(t)$ is the noise modeled as an AWGN with unit variance. At the integrated receiver, the received RF signal $r(t)$ is converted to a direct current (DC) signal $i_{\mathrm{DC}}(t)$ by a rectification circuit. This signal is dynamically split, into two streams with power ratio $1 - \alpha(t)$ for energy harvesting and $\alpha(t)$ is sampled and digitalized by an analog-to-digital converter (ADC) for further information decoding, where $0 < a(t) < 1$. Then, the DC output of the low pass filter[1] (LPF) is [6]

$$i_{\mathrm{DC}}(t) = \left| \sqrt{E_{\mathrm{ave}} h} x(t) + n_1(t) \right|^2 + n_2(t), \quad (4)$$

where $n_2(t)$ is the noise added from the rectifier, modeled as an AWGN with unit variance. In order to reduce the energy requirements for information decoding and jointly maximize the power split for energy harvesting, we consider $\alpha(t) \to 0$ [5]. Furthermore, in practice, the antenna noise power is much smaller than the rectifier noise power, thus it can be omitted ($n_1 \to 0$). Assuming that the symbol period is one and by normalizing $n_2(t)$, the channel at the information decoder can be equivalently viewed as a power signal and is given by

$$y = E_{\mathrm{ave}} h x^2 + n_2, \quad (5)$$

where x denotes the signal power, y the channel output, h the power gain of the channel and n_2 the rectifier noise.

The harvested energy denoted by Q in Joule is given by [5]

$$\begin{aligned} Q &= \zeta \mathbb{E}[i_{\mathrm{DC}}(t)] = \zeta \mathbb{E}[E_{\mathrm{ave}} h x^2] \\ &= \zeta \int_{E_{\mathrm{sens}}}^{\infty} \frac{h}{E_{\mathrm{ave}}} \exp\left(-\frac{h}{E_{\mathrm{ave}}}\right) dh \\ &= \zeta (E_{\mathrm{ave}} + E_{\mathrm{sens}}) \exp\left(-\frac{E_{\mathrm{sens}}}{E_{\mathrm{ave}}}\right), \end{aligned} \quad (6)$$

which follows from the fact that h is exponentially distributed with mean E_{ave}; E_{sens} denotes the level of power sensitivity at the receiver and $0 < \zeta \leq 1$ is the conversion efficiency, which we assume throughout this work $\zeta = 1$. Here we ignore the energy from the noise assuming that it is negligible. In the case, where we do not apply a level of power sensitivity at the receiver side, i.e. $E_{\mathrm{sens}} = 0$, the harvested energy from (6) results in $Q = E_{\mathrm{ave}}$.

III. SBS Decoding

In this section, we study SBS detection with the use of maximum likelihood estimation. Integral forms for the SER of all the considered schemes are derived.

A. Performance Analysis

The total pairwise error probability regarding adjacent symbols, can be calculated considering two independent events A and B. The event A is characterized by the fact that the received signal y is negative. In such a case, the integrated receiver does not proceed neither with information decoding nor with energy harvesting. As a consequence, we have an outage no matter what was the trasmitted symbol. Thus, the pairwise error probability given that the event A holds, equals the probability of $E_{\mathrm{ave}} h x_i^2 + n_2 \leq 0$ for all x_i, given by

$$P_{\mathrm{pair}}(A) = \frac{1}{M} \sum_{i=1}^{M} P(n_2 \leq -E_{\mathrm{ave}} h x_i^2)$$

[1]For reasons of simplification, we assume a linear model for the energy harvested. Non-linear models will be considered for future work.

$$= \frac{1}{M}\int_0^{\infty} \frac{1}{2}\exp(-h)\left(M + \sum_{i=1}^{M} \text{erf}(-E_{\text{ave}} h x_i^2)\right) dh, \quad (7)$$

which follows by substituting the cumulative distribution function of the AWGN term n_2 [14, Eq. (2.3-11)] and integrating for all the possible values of h.

Respectively, the event B is characterized by the fact that the received signal y is positive. Given this and in contrast to the event A, we are not always in outage. More specifically, the pairwise error probability for adjacent symbols given that the event B holds and assuming that symbol x_i was transmitted, is defined by

$$P_{\text{pair}}(B) = \frac{1}{MP(B)} \sum_{i=1}^{M} P(e_{x_i}), \quad (8)$$

where $P(e_{x_i})$ is the probability of error, that the receiver wrongly decides on x_{i+1} or x_{i-1} symbol, while x_i was transmitted. Thus,

$$\sum_{i=1}^{M} P(e_{x_i}) = \sum_{i=1}^{M} \left[P(e_{i\to i+1}) + P(e_{i\to i-1})\right], \quad (9)$$

where $P(e_{i\to i+1})$ and $P(e_{i\to i-1})$, denote the pairwise error probability on deciding symbol x_{i+1} or x_{i-1}, respectively, when symbol x_i was transmitted and are given in the Appendix.

Furthermore, $P(B)$ represents the probability that the received signal y is positive, i.e. $E_{\text{ave}} h x_i^2 + n_2 > 0$, for any trasmitted $x_i \in \{1d, 2d, \ldots, Md\}$. Following the steps for the calculation of $P_{\text{pair}}(A)$ in (7), we can similarly estimate

$$P(B) = \frac{1}{M}\int_0^{\infty} \frac{1}{2}\exp(-h)\left(M - \sum_{x_i=1}^{M} \text{erf}(-E_{\text{ave}} h x_i^2)\right) dh. \quad (10)$$

By substituting (9) and (10) in (8), we can derive the total pairwise error for the integrated receiver, referring to a SBS detection as

$$P_{\text{SER\_sbs}} = P_{\text{pair}}(A) + P_{\text{pair}}(B). \quad (11)$$

B. Optimized Performance Analysis

In this subsection, we study the optimization of the integrated symbol by symbol decoder (OSBS), targeting the minimization of $P_{\text{SER\_sbs}}$. In order to achieve this, we consider that our energy pulse based symbol alphabet is no longer based on equi-spaced amplitudes. We thus define a new constrained non linear optimization problem. We set an objective function that we need to minimize, subject to specific non linear equalities and linear inequalities expressed as

$$\begin{aligned} P_{\text{OSBS}} &= \min_{x_i} P_{\text{SER\_sbs}} \\ \text{subject to } & \mathbb{E}[x^2] = 1, \\ & f_Y(y_{x_i}) = f_Y(y_{x_i+1}), \quad i \in \{1, \ldots, M-1\}, \\ & x_i \le x_{i+1}, \quad i \in \{1, \ldots, M-1\}, \end{aligned} \quad (12)$$

where $f_{\text{Y}}(y_{x_{\text{i}}})$ denotes the probability density function (pdf) of the received signal y when x_i is transmitted, $f_{\text{Y}}(y_{x_{\text{i}+1}})$ denotes the pdf of the received signal y, when x_{i+1} is transmitted and are given in the Appendix. Such an optimization problem, can be solved reliably and efficiently with existing numerical tools, such as *fmincon* in Matlab [11], which employs the interior-point method.

C. Optimized Performance Analysis with Power Sensitivity

Applying a level of power sensitivity in the integrated receiver, we target a more sophisticated scenario of the symbol by symbol detection (OPS). The integrated receiver proceeds to information decoding and energy harvesting, if and only if the received power of the DC signal is higher than a given sensitivity level. Such an assumption, results in two new events A' and B'; A' is characterized by the fact that $E_{\text{ave}} h x_i^2 + n_2 \le E_{\text{sens}}$, and B' from the fact that $E_{\text{ave}} h x_i^2 + n_2 > E_{\text{sens}}$. Following the steps which are analytically described in Section III-A, we can calculate the new SER of the system.

IV. Sequential Decoding

In this section, we exploit the coherence time of the channel over N transmitted energy pulses, and study sequential detection. With the use of such a detection scheme, the performance of the integrated SWIPT receiver is enhanced, in terms of SER. However, in order to keep a low computational complexity, our study focuses in more sophisticated techniques. Specifically:

- Our first step is focused on detecting a subsequence of the transmitted energy pulses, with the use of GLRT-MLSD. In this way, we derive a simple decision rule for information decoding, that is independent of the channel gain, succeeding non-coherent detection.
- Secondly, with the use of Viterbi-type trellis-search algorithm, we manage to reduce the search complexity of the proposed decision metric.
- Finally, with the use of SS-ST, we eliminate the error floor.

At the end of this section, we provide integral forms for the upper bounds derived, regarding the SER performance of our proposed integrated SEQ-MLSD decoder and the conventional power-splitting SWIPT receiver.

A. Sequence Detection

We consider a subsequence of L immediate past symbols, out of the entire transmitted sequence with coherence length N. At time t, the transmitted data subsequence is denoted by $\mathbf{x}(t, L) = [x(t-L+1), \ldots, x(t)]$, where $x(t) \in \{1d, 2d, \ldots, Md\}$ for any time t. Similarly, $\mathbf{y}(t, L) = [y(t-L+1), \ldots, y(t)]$ and $\mathbf{n}_2(t, L) = [n_2(t-L+1), \ldots, n_2(t)]$ are used to denote the corresponding received signal subsequence and noise subsequence, respectively. For the sake of simplicity, we drop the index terms t and L and denote the vectors $\mathbf{x}, \mathbf{y}$ and $\mathbf{n}_2$. Thus, the received signal is modeled as

$$\mathbf{y} = E_{\text{ave}} h \mathbf{x} + \mathbf{n}_2. \quad (13)$$

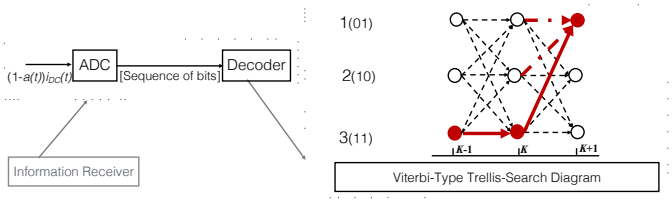

Fig. 2. Viterbi-type trellis-search diagram for integrated SEQ-MLSD decoder.

Having defined our subsequence, we target on a detection scheme that will be independent from the channel gain h. A GLRT-MLSD decoder is used, in order to jointly decide on h and $\mathbf{x}$, that maximize $p(\mathbf{y}|\mathbf{x},h)$, which is the conditional pdf of $\mathbf{y}$. With the use of maximum likelihood, h is estimated conditioned on a hypothesized data subsequence $\mathbf{x}$. Then, with the proper substitutions and computations, the desicion rule is further simplified and finally reduced to [8, sec.IV]

$$\tilde{\mathbf{x}} = \arg\max_{\mathbf{x}} \frac{(\mathbf{y}\cdot\mathbf{x})^2}{\|\mathbf{x}\|^2}, \tag{14}$$

where $\tilde{\mathbf{x}}$ denotes the detection result on subsequence $\mathbf{x}$. We notice that the CSI is not required, something that is crucial to our proposed approach.

B. The Viterbi-Type Trellis-Search Algorithm

In principle, to implement the above metric, one has to compare M^L possible subsequences and choose the one with the higher metric value. With the use of Viterbi-type trellis-search algorithm, the search complexity can be reduced to a very low level that is independent of the observation window length L [8]. As can be seen from Fig. 2, at each time t, the algorithm with the use of (14):

- computes the metrics of all the hypothesized sequences arriving at a node,
- saves the sequence with the higher metric value,
- discards the sequence with the lower metric value.

This is repeated for all paths entering the same node, and the path with the largest metric is saved as the survivor one. As shown with the red solid line in Fig. 2, the decision on a symbol is made only when the tails of all survivors have merged at a node. Though it has to be noticed, that the search complexity increases quadrically as M grows, since for each symbol detection, one has to compute the decision metrics of all M^2 paths.

C. The SS-ST Method

With the use of SS-ST, we enhance our integrated SEQ-MLSD decoder, by overcoming the error floor problem which exists in values of $M > 2$ [9]. In SS-ST the decision metric selectively uses the L most recent received signals that have been detected to carry symbol Md, before the last merge node. Using signals with the highest power to estimate the channel state [8], defines SS-ST as a high efficient technique. Alternatively, without the use of SS-ST, the decision rule is based on the last L immediate received signals. The possibility that a decision on a symbol has not been made, in other words the tails of all survivors have not merged at a node, causes an error floor.

D. Performance Analysis

The pairwise error probability of a GLRT-MLSD decoder when $L \to \infty$, is given by [8, Eq. (34)]. With the proper substitutions, taking into account the characteristics of our proposed integrated SEQ-MLSD decoder and proceeding with an integration over all the possible values of h, the average pairwise error for adjacent symbols is given by [13]

$$\begin{aligned} P_{\text{SER\_pair}} &= \mathbb{E}\left[\frac{1}{2}\text{erfc}\left(\frac{hE_{\text{ave}}\sqrt{d}}{2\sqrt{2}\sigma^2}\right)\right] \\ &= \int_0^\infty \frac{1}{2}\text{erfc}\left(\frac{hE_{\text{ave}}\sqrt{d}}{2\sqrt{2}\sigma^2}\right)\exp\left(-h\right)dh. \end{aligned} \tag{15}$$

As the transmitted symbols and consequently the energy levels M, increase to more than 2, the probability that y will be closer to some other x_j than to x_i, is upper bounded by the sum of the pairwise error probabilities to all the other signals $x_j \neq x_i$. We herein, define the upper bound of the probability of a union of events [14]

$$P_{\text{SER\_seq}} = \frac{1}{M}\sum_{x_i\in A} P(e_{x_i}) \leq \frac{2(M-1)}{M} P_{\text{SER\_pair}}, \tag{16}$$

where $P(e_{x_i})$ is the probability of error given that x_i was transmitted.

Conventional Power-Splitting SWIPT Receiver: For the sake of comparison, we additionally provide a SWIPT solution with the use of a separated architecture (conventional decoder) [12]. In this case, the received signal is split in two portions before being converted to a DC signal, while still is in the RF band. The transmitted signal uses pulse amplitude modulation (PAM), with M constellation points $x_i \in \{\pm\frac{1}{2}d_{\min}, \ldots, \pm\frac{M-1}{2}d_{\min}\}$, where $d_{\min}$ is the minimum distance between two symbols as referred in [14, Ch. 4.3-1]. The average energy per bit transmitted is E_{bavg}, while at the transmitter side a baseband signal $x(t)$ is transmitted as in the case of the integrated receiver. The RF signal is then transmitted over a Rayleigh fading channel with gain h. At the receiver side, a power ratio α of the signal, is used for SBS decoding with the use of maximum likelihood. The remaining $1-\alpha$ portion is led to an energy receiver, which proceeds to a DC conversion as described in [5] and energy harvesting. As in the case of integrated SEQ-MLSD decoder, the noise power from the antenna is omitted. Thus, the average SER over all possible values of h is [14, Eq. (4.3-5)]

$$\begin{aligned} P_{\text{SER\_PAM}} &= \frac{(M-1)}{M} \\ &\times \int_0^\infty \text{erfc}\left(\sqrt{\frac{3\log_2 M}{M^2-1}\frac{\alpha E_{\text{ave}} h E_{\text{bavg}}}{\sqrt{2}}}\right)\exp\left(-h\right)dh. \end{aligned} \tag{17}$$

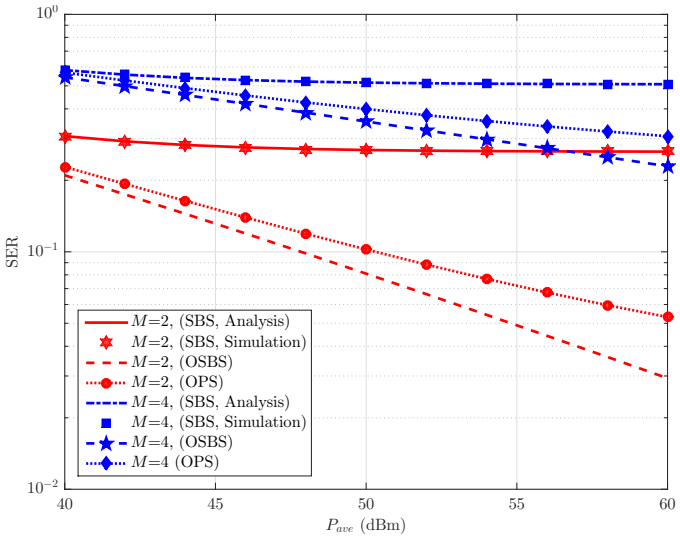

Fig. 3. Performance of integrated receiver over different number of energy levels M, for all considered schemes; SBS, OSBS and OPS with an indicative example of $E_{\text{sens}} = 0.5E_{\text{ave}}$.

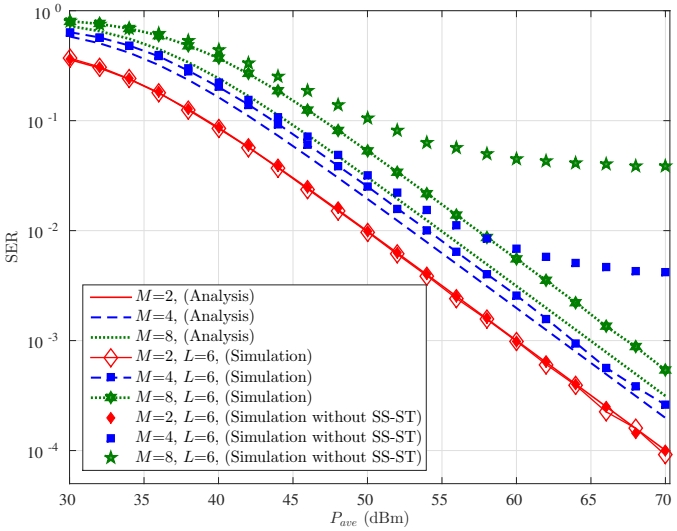

Fig. 4. Performance of our proposed integrated SEQ-MLSD decoder over different number of energy levels M, sequence length $L = 6$, with and without the use of SS-ST.

Taking into account the $(1-\alpha)$ factor and with the use of (6), the energy harvested can be expressed as

$$Q_{\text{PAM}} = (1-\alpha)E_{\text{ave}}. \tag{18}$$

It is clear that the energy harvested from a conventional decoder (Q_{PAM}) is always less than the energy harvested in a SBS detection scheme with $E_{\text{sens}} = 0$; equality holds for $\alpha \to 0$.

In the following sections, analysis and simulation results are presented as a benchmark to our proposed integrated SEQ-MLSD decoder.

V. Numerical Results

Computer simulations are carried out in order to evaluate the performance of an integrated receiver achieving SWIPT, for the aforementioned non-coherent detection schemes. In Fig. 3, we present the behavior of SER regarding SBS detection, OSBS, where the pattern of the transmitted energy pulses is optimized and OPS, where a level of power sensitivity is applied at the receiver. As expected, with the increase of E_{ave} and the optimization, the performance of SER is enhanced, while by applying a level of power sensitivity at the receiver, the performance of SER deteriorates.

In Fig. 4, we study the performance of SEQ-MLSD decoder, for a variety of energy levels, with the use of SS-ST and $L = 6$. These results, are compared to a similar system model without the use of SS-ST and to the union bound of the pairwise error probability, as this is described in (16). In comparison to the SBS detection in Fig. 3, the SER follows the same behavior when E_{ave} and M increase, but with remarkably lower values. One more key observation, is the fact that with the use of SS-ST, the SER is enhanced for the same M energy levels, while at the same time the error floor is eliminated. Furthermore, as the number of energy pulses M increases, due to the existence of more than one pairwise error, the simulation results are compared to the union bound, resulting thus to a higher divergence between simulation and numerical results.

In Figs. 5 and 6, we compare the performance of our proposed integrated SEQ-MLSD decoder with the conventional one. It can be noticed that for higher values of the average transmitted power e.g. $E_{\text{ave}} = 50$ dBm, our proposed integrated SEQ-MLSD decoder improves remarkably its SER performance. Also, in both figures, it is clear that the conventional decoder achieves a better SER performance than our proposed integrated SEQ-MLSD, for values of $\alpha \geq 0.1$, having as a direct consequence the severe degradation of the energy harvested. For values of $\alpha < 0.1$, our proposal outperforms the conventional one both in terms of SER and energy harvested.

VI. Conclusion

In this paper, we study an integrated SWIPT receiver, with the use of non-coherent detection schemes. We investigate the performance in terms of SER, while with the use of sophisticated techniques we succeed to enhance it without deteriorating the energy harvested. First, we examine a SBS detection scheme; optimization on the pattern of the transmitted energy pulses is carried out, with and without a level of power sensitivity at the receiver. In addition, relying on the coherence time of the channel over N transmitted energy pulses, we exploit sequential detection and propose our integrated SEQ-MLSD decoder. With the use of Viterbi-type trellis search algorithm, we simplify the complexity of our proposed sequential decoder, while with SS-ST we overcome the error floor problem. Simulation and theoretical results are consistent, corroborating our proposed solution. Our SEQ-MLSD decoder succeeds enhanced SER without degrading the energy harvested, compared to a SBS integrated decoder and a conventional power-splitting SWIPT receiver.

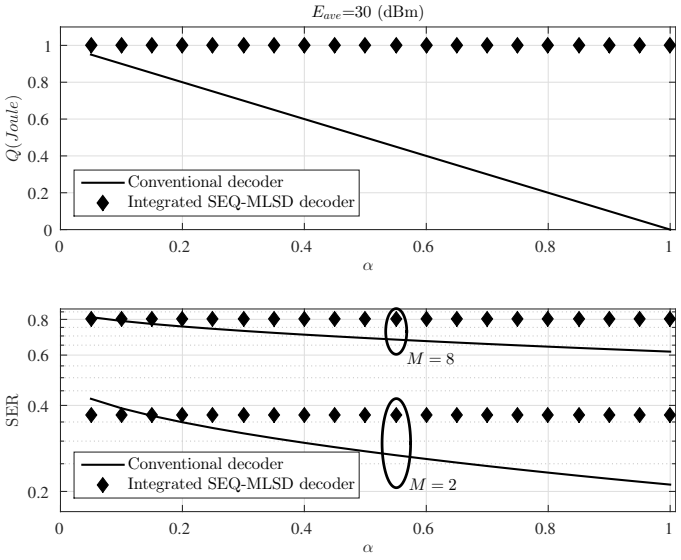

Fig. 5. Energy harvested and SER versus α, for $E_{\rm ave} = 30$ dBm.

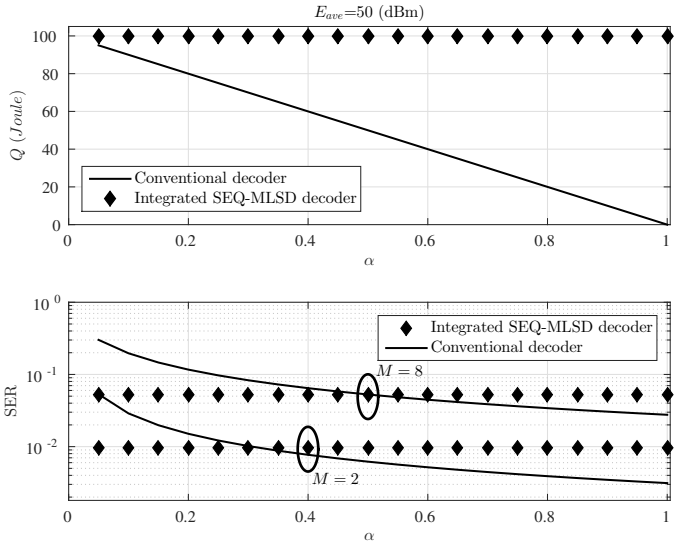

Fig. 6. Energy harvested and SER versus α, for $E_{\rm ave} = 50$ dBm.

APPENDIX

The probability of error deciding symbol x_{i+1} when symbol x_i is transmitted, is directly related with the probability that the received signal $y_{x_{i+1}}$ is higher than y_{x_i}, which results in

$$f_{\rm Y}(y_{x_{\rm i}}) \leq f_{\rm Y}(y_{x_{\rm i+1}}), \tag{19}$$

where $f_{\rm Y}(y_{x_{\rm i}})$ denotes the pdf of the received signal y. From (5), the channel power gain follows an exponential distribution and the rectifier noise follows a normal distribution. Therefore, y follows an exponentially modified Gaussian (EMG) distribution, with pdf [15]

$$\begin{aligned} f_Y(y_{x_i}) =& \frac{\lambda_i}{2} \exp\left(\frac{\lambda_i}{2}\left(2\mu + \lambda_i\sigma^2 - 2y_{x_i}\right)\right) \\ & \times \operatorname{erfc}\left(\frac{\mu + \lambda_i\sigma^2 - y_{x_i}}{\sqrt{2}\sigma}\right), \end{aligned} \tag{20}$$

where μ and σ^2 are the mean and the variance of the Gaussian component, respectively. In our case $\mu = 0$ and $\sigma^2 = 1/2$, since we are interested only in the real part of the complex Gaussian noise n_2. Furthermore, we assume that the symbols x_i are equally probable transmitted and λ_i is the rate of the exponential component, which in our case is $\lambda_i = \frac{1}{(2E_{\rm ave}x_i^2)}$. In order to define $P(e_{i\to i+1})$, when $i < M$, we need to calculate the probability of (19). Consequently,

$$P(e_{i\to i+1}) = \int_{c_1}^{\infty} f_Y(y_{x_i}) dy_{x_i}, \tag{21}$$

where c_1 is derived when equality holds for (19). In other words, c_1 returns the value of y, where the pdfs of the received signals for the transmitted symbols x_i and x_{i+1} intersect. Respectively, for $i > 1$, $P(e_{i\to i-1})$ can be calculated as

$$P(e_{i\to i-1}) = \int_{0}^{c_2} f_Y(y_{x_i}) dy_{x_i}, \tag{22}$$

subject to $f_{\rm Y}(y_{x_{\rm i}}) \leq f_{\rm Y}(y_{x_{\rm i-1}})$ and given that c_2 is derived when equality holds.

REFERENCES

[1] I. Krikidis, S. Timotheou, S. Nikolaou, G. Zheng, D. W. K. Ng, and R. Schober, "Simultaneous wireless information and power transfer in modern communication systems," *IEEE Commun. Mag.*, vol. 52, pp. 104–110, Nov. 2014.

[2] T. Taleb and A. Kunz, "Machine type communications in 3GPP networks: Potential, challenges, solutions," *IEEE Commun. Mag.*, vol. 50, pp. 178–184, Mar. 2012.

[3] L. R. Varshney, "Transporting information and energy simultaneously," in *Proc. IEEE Int. Symp. Inf. Theory*, Toronto, Canada, pp. 1612–1616, July 2008.

[4] P. Grover and A. Sahai, "Shannon meets Tesla: Wireless information and power transfer," in *Proc. IEEE Int. Symp. Inf. Theory*, Austin, TX, pp. 2363–2367, June 2010.

[5] X. Zhou, R. Zhang, and C. K. Ho, "Wireless information and power transfer: Architecture design and rate-energy tradeoff," *IEEE Trans. Commun.*, vol. 61, pp. 4757–4767, Nov. 2013.

[6] R. Zhang, L. Yang, and L. Hanzo, "Energy pattern aided simultaneous wireless information and power transfer," *IEEE J. Select. Areas Commun.*, vol. 33, pp. 1492–1504, August 2015.

[7] P. Liu, S. Gazor, Il-M. Kim, and D.I. Kim, "Noncoherent relaying in energy harvesting communication systems," *IEEE Trans. Commun.*, vol. 14, pp. 6940–6954, July 2015.

[8] T. Song and P. Kam, "Efficient direct detection of M-PAM sequences with implicit CSI acquisition for the FSO system," in *Proc. IEEE Global Commun. Conf. Workshops*, Austin, TX, pp. 475-480, Dec. 2014.

[9] D. Papailiopoulos, G. A. Elkheir, and G. N. Karystinos, "Maximum-likelihood noncoherent PAM detection," *IEEE Trans. Commun.*, vol. 61, pp. 1152–1159, Mar. 2013.

[10] W. Liu, X. Zhou, S. Durrani, and P. Popovski, "SWIPT with practical modulation and RF energy harvesting sensitivity," in *Proc. IEEE Int. Conf. on Commun. (ICC)*, Kuala Lumpur, Malaysia, pp. 4430-4436, May 2016.

[11] Matlab and Optimization Toolbox User Guide, Release 2013, The MathWorks, Inc., Natick, Massachusetts, United States.

[12] C.-H. Chang, R. Y. Chang, and F.-T. Chien, "Energy-assisted information detection for SWIPT: Performance analysis and case studies," *IEEE Trans. Signal Inf. Process. Net.*, vol. 2, June 2016.

[13] E. Goudeli, C. Psomas, and I. Krikidis, "Sequential decoding for simultaneous wireless information and power transfer," in *IEEE Int. Conf. on Telecommun. (ICT)*, Limassol, Cyprus, May 2017.

[14] J. G. Proakis and M. Salehi, *Digital Communications*, McGraw-Hill, 5th ed., 1995.

[15] Eli Grushka, "Characterization of exponentially modified Gaussian peaks in chromatography," *Anal. Chem.*, vol. 44, pp. 1733-1738, Sep. 1972.